Recent Changes in Particulate Air Pollution over China Observed from Space and the Ground: Effectiveness of Emission Control

JINTAI LIN,[§,†] CHRIS P. NIELSEN,[†] YU ZHAO,[†] YU LEI,[†] YANG LIU,[‡] AND MICHAEL B. MCELROY*,[†]

Department of Atmospheric and Oceanic Sciences, School of Physics, Peking University, Beijing, 100871, China, School of Engineering and Applied Sciences and Harvard China Project, Harvard University, 19 Oxford Street, Cambridge, Massachusetts 02138, and Department of Environmental and Occupational Health, Emory University, Rollins School of Public Health, 1518 Clifton Road NE, Atlanta, Georgia 30322

The Chinese government has moved aggressively since 2005 to reduce emissions of a number of pollutants including primary particulate matter (PM) and sulfur dioxide (SO_2), efforts inadvertently aided since late 2008 by economic recession. Satellite observations of aerosol optical depth (AOD) and column nitrogen dioxide (NO_2) provide independent indicators of emission trends, clearly reflecting the sharp onset of the recession in the fall of 2008 and rebound of the economy in the latter half of 2009. Comparison of AOD with ground-based observations of PM over a longer period indicate that emission-control policies have not been successful in reducing concentrations of aerosol pollutants at smaller size range over industrialized regions of China. The lack of success is attributed to the increasing importance of anthropogenic secondary aerosols formed from precursor species including nitrogen oxides (NO_x), non-methane volatile organic compounds (NMVOC), and ammonia (NH_3).

1. Introduction

Aerosols have a significant impact not only on climate (*1–3*) but also on public health (*4*). The impact is particularly important for particles of small sizes, formed for example from precursor chemicals including sulfur dioxide (SO_2), nitrogen oxides (NO_x), non-methane volatile organic compounds (NMVOC), and ammonia (NH_3). These particles, which are generally hydroscopic and reflective, can have a significant impact on the energy budget of the climate system, responsible for negative radiative forcing offsetting positive forcing from greenhouse gases. Given their small sizes, they can penetrate readily into human lungs triggering a variety of respiratory and cardiovascular problems. Sulfate and nitrate aerosols make an important contribution also to the phenomenon of acid deposition

with negative impacts not only on agriculture but also on natural ecosystems (*5*).

The Chinese government has strong incentives to reduce emissions of aerosols and precursors. China is a major source region of anthropogenic aerosols as a consequence of fast industrialization and urbanization, the reliance of the Chinese economy on coal and relatively weak emission controls (*5–8*). The resulting high aerosol loadings (*9, 10*) and strong acid deposition (*5*) have posed a major domestic environmental problem. To tackle these issues, China has taken aggressive steps since 2005 to reduce emissions of primary aerosols and SO_2 (see Supporting Information section 1).

Observations from space and in situ can be used to provide information on aerosols over source regions. Here we use such data to evaluate the effect of recent emission controls on aerosol loading in East China (see Figure 1a for region specifications) over the course of Oct 2004–Dec 2009. Data employed here include daily aerosol optical depth (AOD) at 342.5 and 483.5 nm measured by the Ozone Monitoring Instrument (OMI) onboard the Aura satellite, daily AOD at 550 nm derived from the MODerate Resolution Imaging Spectroradiometer (MODIS) onboard the Aqua satellite, and surface observations in 66 major cities for daily mean mass concentrations of particulate matter with diameters not more than 10 μm ([PM_{10}]). In addition, monthly mean tropospheric vertical column densities (VCDs) of nitrogen dioxide (NO_2) retrieved from OMI are exploited to estimate changes in emissions of NO_x.

2. Descriptions of Atmospheric Measurements

This section briefly describes various atmospheric measurements used in the present study. More detailed analysis is presented in Supporting Information section 2.

The OMI AOD data were taken from the daily level-3 data set OMAEROe (available at http://disc.sci.gsfc.nasa.gov/ Aura/data-holdings/OMI/omaeroe_v003.shtml) with a horizontal resolution of 0.25° lat × 0.25° long based on the level-2 retrieval using the multiwavelength algorithm, OMAERO (*11, 12*). Validation of OMAERO has been discussed by Curier et al. (*13*), Brinksma et al. (*14*), and Livingston et al. (*15*). The version of the product used here is derived using surface albedo retrieved from OMI, an update from previous versions (*13–15*) employing surface albedo retrieved from the Multiangle Imaging SpectroRadiometer (MISR), and is expected to contain smaller errors associated with surface albedo (J. P. Veefkind, personal communication). The detailed methodology for generating the OMAEROe data set can be found at the online readme file (*16*). AOD values for five wavelengths are retrieved simultaneously by the algorithm, ranging from 342.5 to 483.5 nm, and those at 342.5 and 483.5 nm are employed in this study. Comparison of OMI AOD with ground-based AOD measurements is available in Supporting Information section 4.

The Aqua MODIS AOD data were taken from the Deep Blue product of the daily level-3 data set at 1° lat × 1° long for product Collection 5.1, MOD08_D3.051 (available at http://gdata1.sci.gsfc.nasa.gov/daac-bin/G3/gui.cgi?instance_id=MODIS_DAILY_L3) (*9, 17, 18*). The MODIS instrument is dedicated to monitor aerosols. It passes China ~10 min ahead of OMI. As compared to OMI, it has a smaller footprint of 10 km × 10 km consisting of 400 fine pixels sized at 0.5 km × 0.5 km (*18*), thus its measurements are less subjective to cloud contamination. It, however, may be more sensitive to errors in surface albedo as a limitation of the longer wavelength and requires the presence of dark dense vegeta-

* Corresponding author phone: (617)495-4359; e-mail: mbm@ seas.harvard.edu.
§ Peking University.
† Harvard University.
‡ Emory University.
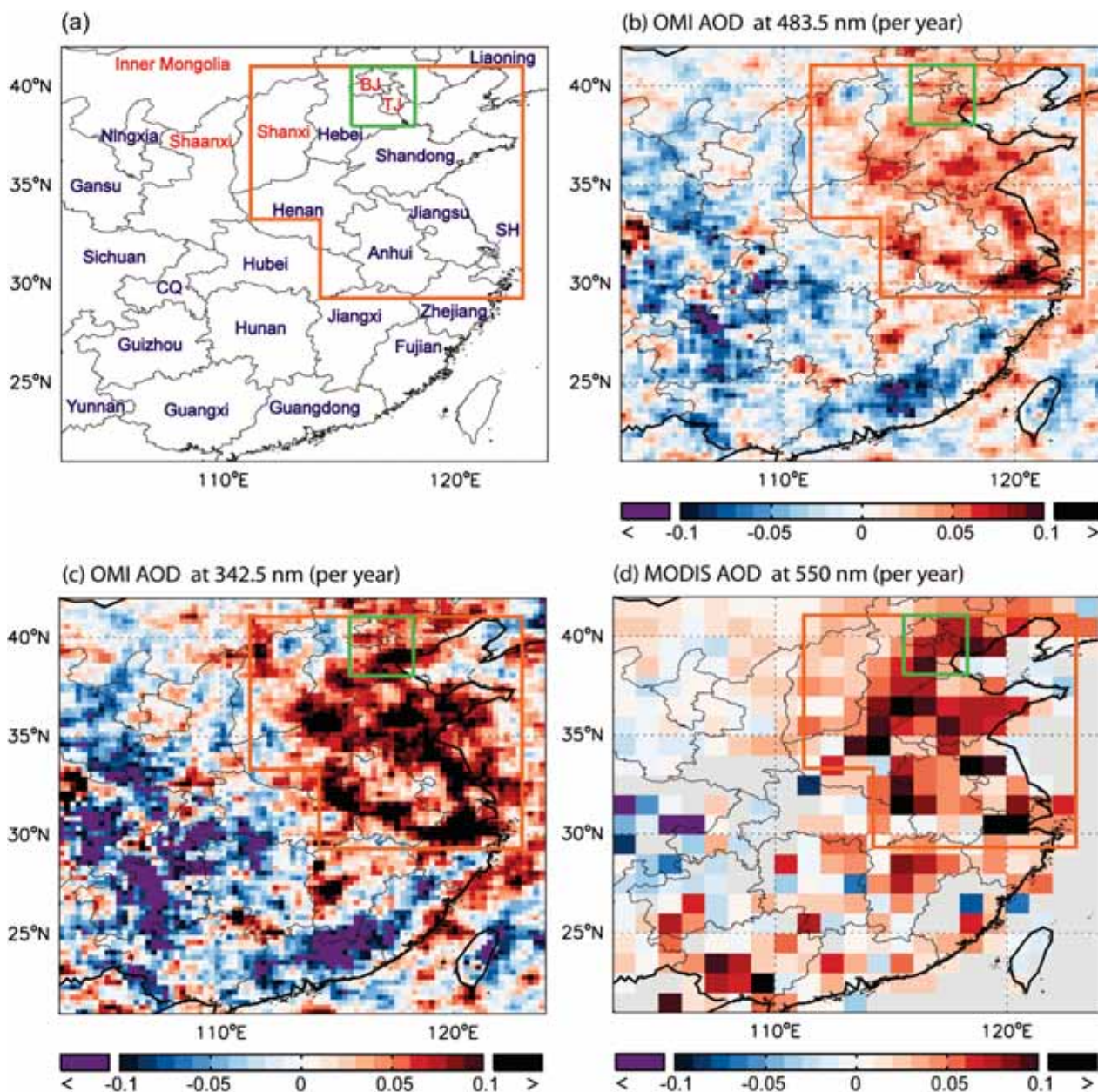
FIGURE 1. Regional specifications based on linear trend analysis. (a) Definition of East China (103°E-124°E, 21°N-42°N; the entire domain) and its subregion 'northeast' as bounded by brown lines. The Beijing-Tianjin area, part of the northeastern region, is bounded by green lines. Also shown are provinces and province-level municipalities (Beijing ('BJ'), Tianjin ('TJ'), Shanghai ('SH'), and Chongqing ('CQ')) in East China. Jurisdictions in red are mentioned in the paper. (b-d) Interannual trends of AOD over Oct 2004-Sep 2008 (prior to the economic downturn) derived with a simple fit using linear regression (see Supporting Information section 3); results are not available in areas shown in gray color.

tion (DDV) pixels in each 10 km × 10 km region (17). Combining AOD products from OMI and MODIS reduces the effect of retrieval errors in analyzing trends of aerosols.

The optical properties of aerosols are very sensitive to their sizes relative to the wavelength of radiation, and small (large) aerosols have a larger contribution to the extinction of light at short (long) wavelengths. At the three relatively short wavelengths analyzed here, the AOD values are particularly sensitive to $PM \leq 2.5 \, \mu m$ ($PM_{2.5}$), which has a mode diameter not more than $1 \, \mu m$, than to larger aerosols (19−22). These aerosols are derived both from emissions at the surface and from secondary formation in the atmosphere. Secondary aerosols are normally much smaller than $2.5 \, \mu m$, including secondary inorganic (sulfate, nitrate, ammonium) and organic aerosols (19, 20, 22). They

make a major contribution to AOD at the short wavelengths analyzed in this study, especially for OMI AOD at 342.5 nm. Particles larger than $2.5 \, \mu m$ are derived typically from surface emissions, including natural dust transported from western China and anthropogenic dust released from industrial processes and urban activities (23−25). They make an important contribution to the mass of PM_{10} in China but normally have a much smaller impact on AOD values analyzed here (19−22). (Effects of large dust aerosols during natural dust events in spring that are potentially important for AOD are discussed in Supporting Information section 5.) Thus the AOD data offer valuable information specifically on the abundance of $PM_{2.5}$. It is noted that the MODIS product has been used to evaluate mass concentrations of $PM_{2.5}$ near the surface (20, 26).

Daily mean mass concentrations of ground-level PM_{10} ($[PM_{10}]$) were derived from the Air Pollution Index (API) data from the Ministry of Environmental Protection (MEP) of China (http://datacenter.mep.gov.cn/TestRunQian/air_dairy_en.jsp). The API records for previous years (2000−2006) have been used to study aerosol loadings and their impacts on meteorology in China (27−31). The conversion from API scores to $[PM_{10}]$ is discussed in Supporting Information section 2.

Tropospheric VCDs of NO_2 were taken from the monthly level-3 data set retrieved by the Royal Netherland Meteorological Institute (KNMI) (available at http://www.temis.nl/airpollution/no2col/no2regioomimonth_col3.php) (32). The product has been used widely to evaluate emissions of NO_x in different parts of the world (33−36). The monthly mean data were provided at a resolution of 0.125° lat × 0.125° long; they have been averaged over a grid of 0.25° lat × 0.25° long for consistency with the OMI AOD data.

Concentrations of aerosols vary significantly both in time and space as a consequence of changes in a variety of factors including emissions of aerosols and precursors, atmospheric lifetimes of aerosols, and meteorological conditions. To evaluate the interannual trends of AOD and $[PM_{10}]$, a 365-day moving average was applied to the daily data to eliminate the effect of temporal variations within a year (see Supporting Information section 3). Similarly, a 12-month moving average was applied to the VCDs of NO_2 data to remove the seasonal variability.

3. Results and Discussion

Analysis of the AOD data indicates an approximately linear trend over the initial four years, Oct 2004−Sep 2008. (The behavior as we show later is more complicated since late 2008 reflecting the influence of the economic recession.) A simple fit for the interannual trend, derived by linear regression on the moving averaged data over the first four years, results in trends of rapid growth in the northeastern region of East China that are consistent across the three AOD products (Figure 1b-d). Densely populated, this region has for decades been under significant industrial development and urbanization and is the main source region of anthropogenic air pollutants of China (7, 23, 37−39). Over the interior regions, interannual trends of AOD are not consistent between OMI and MODIS, attributed to the lower data coverage (Supporting Figure S4) and retrieval errors in individual products. Further study is needed to fully understand the causes of the differences and the real trends of AOD in these regions. We propose in what follows to focus on the northeastern region.

A general downward trend in $[PM_{10}]$ is observed over the northeastern region during the initial period contrasted by an upward trend in AOD (Figures 2a and 3a). Across the 37 cities within the region, mean $[PM_{10}]$ decreased from ~107 μg/m3 to ~96 μg/m^3, while OMI AOD at 483.5 nm increased from a minimum value of ~0.96 to a level of ~1.08, OMI AOD at 342.5 nm increased from ~1.46 to ~1.68, and MODIS AOD increased from ~0.72 to ~0.86. Similar increases are found for regional mean AOD.

A possible explanation of the opposite trends between $[PM_{10}]$ and AOD can be given as the varying effectiveness of emission controls addressing primary aerosols and secondary aerosol precursors in China. First, as presented in more detail in Supporting Information section 1, most national control efforts to date have targeted emissions of primary PM and SO_2. Approximately 60% of anthropogenic emissions of PM in 2005 are derived from three main sources including cement production, coal combustion for power generation, and biofuel burning for residential use (Supporting Figure S1). The recent controls on these sources are estimated to have
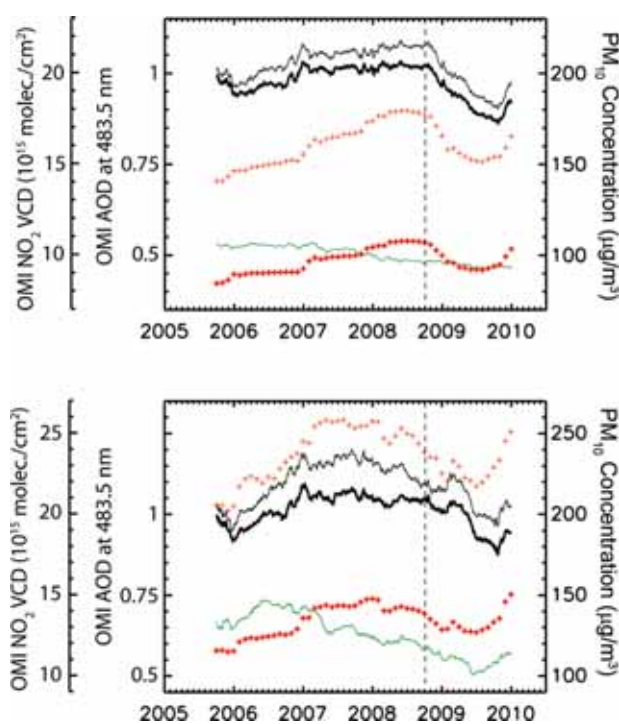
FIGURE 2. Changes in daily data for OMI AOD (at 483.5 nm) and $[PM_{10}]$ and in monthly data for OMI NO_2 VCD during Oct 2004-Dec 2009. The thick black line denotes the regional mean AOD from OMI; the thin black line denotes the mean of OMI AOD sampled in the cities with $[PM_{10}]$ measurements. The thin green line denotes the mean of $[PM_{10}]$ measurements. The thick red '+' line denotes the regional mean NO_2 VCD from OMI; the thin red '+' line denotes the mean NO_2 VCD sampled in the cities with $[PM_{10}]$ measurements. There are 37 and 2 cities with $[PM_{10}]$ measurements in the two regions, respectively. Data shown here are based on a 365-day moving average for OMI AOD and $[PM_{10}]$ and a 12-month moving average for OMI NO_2 VCD, i.e., each data point represents the mean over the prior year (Supporting Information section 3). The dashed vertical line depicts the approximate start of the Chinese economic downturn.

resulted in an overall reduction in emissions of primary PM from 2005 to 2010, with a greater impact on PM larger than 2.5 μm. The targeted control of sulfur in the Eleventh Five-Year Plan (11th FYP) has reportedly led to a decrease in emissions of SO_2 by ~9% from 2005 to 2008 (Supporting Figure S2). In contrast, controls for emissions of other aerosol precursors have been much less strict. As a result, emissions of NO_x are estimated to have grown dramatically in recent years; and emissions of NMVOC and NH_3 are estimated to have increased from 2005 to 2010 by 18% and by up to 10%, respectively (Supporting Information section 1 and Figure S2). The consequent increases in nitrate and ammonium are found to have more than offset the effect of decreases in sulfate on total secondary inorganic aerosols (see model simulations below). Anthropogenic secondary organic aerosols (SOAs) will also have increased as a result of increases in emissions of precursor NMVOC. As controls on large primary aerosols do not have significant impacts on AOD, it is conceivable that increases in anthropogenic secondary aerosols have resulted in overall enhancements in AOD, while $[PM_{10}]$ has reduced as a net result of decreases in primary aerosols and increases in secondary aerosols.

Changes in the source of nitrate aerosols can be inferred from tropospheric VCDs of NO_2 retrieved from OMI. Averaged over the northeastern region, the VCD of NO_2 increased by ~27% during the four years prior to the economic downturn (Figure 2a), a factor of 2−3 larger than the increase in OMI AOD. This implies a significant increase in emissions of NO_x
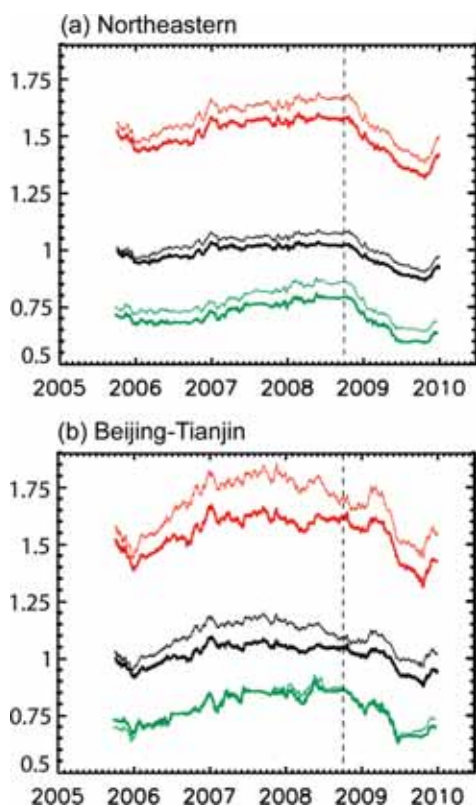
FIGURE 3. Changes in daily AOD values retrieved from OMI and MODIS during Oct 2004-Dec 2009. The black, red, and green lines represent OMI AOD at 483.5 nm, OMI AOD at 342.5 nm, and MODIS AOD at 550 nm, respectively. The think lines denote regional mean AOD; and the thin lines denote AOD averaged over cities with [PM₁₀] measurements. Results for OMI AOD at 485.3 nm are the same as those in Figure 2. There are 37 and 2 cities with [PM₁₀] measurements in the two regions, respectively. Data shown here are based on a 365-day moving average, i.e., each data point represents the mean over the prior year (Supporting Information section 3). The dashed vertical line depicts the approximate start of the Chinese economic downturn.

and, consequently, the concentration of nitrate aerosols, responsible partially for the increase in AOD.

The global chemical transport model (CTM) GEOS-Chem (version 8-03-01; see detailed model descriptions and analyses in Supporting Information section 6) was used to evaluate the net effect of changes in precursor emissions aforementioned on secondary inorganic aerosols (sulfate, nitrate, and ammonium) from Oct 2004−Sep 2005 to Oct 2007−Sep 2008. The 27% increase found in the retrieved VCD of NO_2 was taken to be the increase in emissions of NO_x. (The actual increase in emissions of NO_x may be slightly larger, as discussed in Supporting Information section 6.) Increases in emissions of NH_3 over 2005−2010 were assumed to be linear from year to year so that increases from 2005 to 2008 were estimated to be 6%. Reductions in emissions of SO_2 were taken to be 9% from 2005 to 2008. Model simulations were conducted for Oct 2004, Jan 2005, Apr 2005, and Jul 2005, as representative of the four seasons, for two cases with and without the inclusion of changes in precursor emissions, respectively. It was found that changes in precursor emissions resulted in a net increase in simulated total secondary inorganic aerosols with a 9% increase in AOD and a 12% increase in surface mass concentration. Consistent with our analysis, Zhao et al. (5) suggested that the impact of sulfur control on acid deposition from 2005 to 2010 might be negated by the increase in emissions of NO_x and NH_3 under current policies.

The effect of emission reductions associated with the economic recession that set in during late 2008 and persisted until late 2009 is evident in the AOD and NO_2 VCD data for the northeastern region (Figures 2a and 3a). In particular, regional mean AOD at 483.5 nm from OMI decreased from a value exceeding 1.0 prior to the economic recession to a comparatively low level of 0.87 in late 2009; the reductions are ∼0.24 for OMI AOD at 342.5 nm and ∼0.2 for MODIS AOD. Concurrently, the VCD of NO_2 decreased by about 15%. More recent data, for Oct-Dec 2009, indicate a recovery in both AOD and NO_2 VCD, in agreement with the resumption of growth in the Chinese economy during this period.

The short-term emission restrictions targeting the 2008 Beijing Summer Olympics had an important impact for the Beijing-Tianjin area (part of the northeastern region as defined here), where both AOD and NO_2 VCD decreased after 2007 following an increase in the prior years (Figures 2b and 3b). The reduction is most evident in the data for the cities of Beijing and Tianjin. For example, OMI AOD at 483.5 nm dropped by ∼9% from the 2007 mean to the 2008 mean and NO_2 VCD declined by ∼12% (15−20% for AOD and 20−30% for NO_2 VCD if the summertime values alone are considered).

As discussed in Supporting Information section 5, the conclusions drawn here are relatively insensitive to the influence of changes in meteorological conditions including precipitation, temperature, wind speed, mixing in the boundary layer, and associated changes in biogenic SOAs and natural dust aerosols.

PM_{10} has long been the main focus of aerosol control in China. Acknowledgments of the environmental impacts of small aerosols, however, have been emphasized recently by the Chinese government (http://lianghui2009.people.com.cn/GB/145749/8944981.html; in Chinese). Our analysis shows the increasing importance of small aerosols formed in the atmosphere from anthropogenic sources as industrialization and urbanization advances in China. This supports the proposal of the Chinese government that stricter control measures be implemented to reduce emissions of aerosol precursors for the 12th FYP over 2011−2015 (http://www.sp.com.cn/dlzj/zc/201002/t20100208_146653.htm; http://www.mep.gov.cn/gkml/hbb/bwj/201002/t20100201_185219.htm; in Chinese).

Changes in composition of aerosols may have important consequences on public health also because different constituents of aerosols may have different impacts on respiratory system and cardiovascular mechanisms. This issue can be addressed by further studies.

Supporting Information Available
Analysis of controls and magnitudes of anthropogenic emissions of aerosols and precursors in China; detailed data descriptions and processing for OMI AOD, MODIS AOD, [PM₁₀], OMI NO_2 VCDs, and surface measurements of AOD and meteorological parameters; evaluation of OMI AOD using ground-based AOD measurements; analysis of effects of changes in meteorology, biogenic SOAs and natural dust on total aerosols; and detailed analysis of secondary inorganic aerosols using simulations of GEOS-Chem. This material is available free of charge via the Internet at http://pubs.acs.org.

Literature Cited

(1) IPCC, Summary for Policymakers. In *Climate Change 2007: The Physical Science Basis. Contribution of Working Group I to the Fourth Assessment Report of the Intergovernmental Panel on Climate Change*; Solomon, S., Qin, D., Manning, M., Chen, Z., Marquis, M., Averyt, K. B., Tignor, M., Miller, H. L., Eds.; Cambridge University Press: Cambridge, United Kingdom and New York, NY, USA, 2007.

(2) Seinfeld, J. H.; Carmichael, G. R.; Arimoto, R.; Conant, W. C.; Brechtel, F. J.; Bates, T. S.; Cahill, T. A.; Clarke, A. D.; Doherty, S. J.; Flatau, P. J.; Huebert, B. J.; Kim, J.; Markowicz, K. M.; Quinn, P. K.; Russell, L. M.; Russell, P. B.; Shimizu, A.; Shinozuka, Y.; Song, C. H.; Tang, Y. H.; Uno, I.; Vogelmann, A. M.; Weber, R. J.; Woo, J. H.; Zhang, X. Y. ACE-ASIA - Regional climatic and atmospheric chemical effects of Asian dust and pollution. *Bull. Am. Meteorol. Soc.* **2004**, *85* (3), 367–380.

(3) Mercado, L. M.; Bellouin, N.; Sitch, S.; Boucher, O.; Huntingford, C.; Wild, M.; Cox, P. M. Impact of changes in diffuse radiation on the global land carbon sink. *Nature* **2009**, *458* (7241), 1014–1017.

(4) Pope, C.; Dockery, D. Epidemiology of particle effects. In *Air pollution and health*; Holgate, S. T., Koren, H. S., Samet, J. M., Maynard, R. L., Eds.; Academic Press: San Diego, 1999; pp 673–705.

(5) Zhao, Y.; Duan, L.; Xing, J.; Larssen, T.; Nielsen, C. P.; Hao, J. M. Soil Acidification in China: Is Controlling SO2 Emissions Enough. *Environ. Sci. Technol.* **2009**, *43* (21), 8021–8026.

(6) Streets, D. G.; Bond, T. C.; Carmichael, G. R.; Fernandes, S. D.; Fu, Q.; He, D.; Klimont, Z.; Nelson, S. M.; Tsai, N. Y.; Wang, M. Q.; Woo, J. H.; Yarber, K. F. An inventory of gaseous and primary aerosol emissions in Asia in the year 2000. *J. Geophys. Res., [Atmos.]* **2003**, *108* (D21), 8809.

(7) Zhang, Q.; Streets, D. G.; He, K.; Wang, Y.; Richter, A.; Burrows, J. P.; Uno, I.; Jang, C. J.; Chen, D.; Yao, Z.; Lei, Y. NOx emission trends for China, 1995–2004: The view from the ground and the view from space. *J. Geophys. Res.* **2007**, *112* (D22306), 18 pp.

(8) Zhao, Y.; Wang, S. X.; Duan, L.; Lei, Y.; Cao, P. F.; Hao, J. M. Primary air pollutant emissions of coal-fired power plants in China: Current status and future prediction. *Atmos. Environ.* **2008**, *42* (36), 8442–8452.

(9) Remer, L. A.; Kleidman, R. G.; Levy, R. C.; Kaufman, Y. J.; Tanre, D.; Mattoo, S.; Martins, J. V.; Ichoku, C.; Koren, I.; Yu, H. B.; Holben, B. N. Global aerosol climatology from the MODIS satellite sensors. *J. Geophys. Res., [Atmos.]* **2008**, *113* (D14s07), 18 pp.

(10) Forster, P.; Ramaswamy, V.; Artaxo, P.; Berntsen, T.; Betts, R.; Fahey, D. W.; Haywood, J.; Lean, J.; Lowe, D. C.; Myhre, G.; Nganga, J.; Prinn, R.; Raga, G.; Schulz, M.; Dorland, R. V. Changes in Atmospheric Constituents and in Radiative Forcing. In *Climate Change 2007: The Physical Science Basis. Contribution of Working Group I to the Fourth Assessment Report of the Intergovernmental Panel on Climate Change*; Solomon, S., Qin, D., Manning, M., Chen, Z., Marquis, M., Averyt, K. B., Tignor, M., Miller, H. L., Eds.; Cambridge University Press: Cambridge, United Kingdom and New York, NY, USA, 2007.

(11) Torres, O.; Decae, R.; Veefkind, J. P.; de Leeuw, G. OMI Aerosol Retrieval Algorithm. In *OMI Algorithm Theoritical Basis Document, vol III, Clouds, Aerosols and Surface UV Irradiance, ATBD-OMI-03*; Stammes, P., Noordhoek, R., Eds.; KNMI: De Bilt, Netherlands, 2002; pp 47–71.

(12) Torres, O.; Tanskanen, A.; Veihelmann, B.; Ahn, C.; Braak, R.; Bhartia, P. K.; Veefkind, J. P.; Levelt, P. Aerosols and surface UV products from Ozone Monitoring Instrument observations: An overview. *J. Geophys. Res., [Atmos.]* **2007**, *112* (D24s47), 14 pp.

(13) Curier, R. L.; Veefkind, J. P.; Braak, R.; Veihelmann, B.; Torres, O.; de Leeuw, G. Retrieval of aerosol optical properties from OMI radiances using a multiwavelength algorithm: Application to western Europe. *J. Geophys. Res., [Atmos.]* **2008**, *113* (D17s90), 16 pp.

(14) Brinksma, E. J.; Pinardi, G.; Volten, H.; Braak, R.; Richter, A.; Schonhardt, A.; van Roozendael, M.; Fayt, C.; Hermans, C.; Dirksen, R. J.; Vlemmix, T.; Berkhout, A. J. C.; Swart, D. P. J.; Oetjen, H.; Wittrock, F.; Wagner, T.; Ibrahim, O. W.; de Leeuw, G.; Moerman, M.; Curier, R. L.; Celarier, E. A.; Cede, A.; Knap, W. H.; Veefkind, J. P.; Eskes, H. J.; Allaart, M.; Rothe, R.; Piters, A. J. M.; Levelt, P. F. The 2005 and 2006 DANDELIONS NO2 and aerosol intercomparison campaigns. *J. Geophys. Res., [Atmos.]* **2008**, *113* (D16s46), 18 pp.

(15) Livingston, J. M.; Redemann, J.; Russell, P. B.; Torres, O.; Veihelmann, B.; Veefkind, P.; Braak, R.; Smirnov, A.; Remer, L.; Bergstrom, R. W.; Coddington, O.; Schmidt, K. S.; Pilewskie, P.; Johnson, R.; Zhang, Q. Comparison of aerosol optical depths from the Ozone Monitoring Instrument (OMI) on Aura with results from airborne sunphotometry, other space and ground measurements during MILAGRO/INTEX-B. *Atmos. Chem. Phys.* **2009**, *9* (18), 6743–6765.

(16) README for OMAEROe (OMI Daily L3e for OMAERO). http://disc.sci.gsfc.nasa.gov/Aura/data-holdings/OMI/documents/v003/OMAEROe_OSIPS_README_V003.doc (accessed June 30, 2010).

(17) Remer, L. A.; Kaufman, Y. J.; Tanre, D.; Mattoo, S.; Chu, D. A.; Martins, J. V.; Li, R. R.; Ichoku, C.; Levy, R. C.; Kleidman, R. G.; Eck, T. F.; Vermote, E.; Holben, B. N. The MODIS aerosol algorithm, products, and validation. *J. Atmos. Sci.* **2005**, *62* (4), 947–973.

(18) Levy, R. C.; Remer, L. A.; Tanré, D.; Mattoo, S.; Kaufman, Y. J. Algorithm for Remote Sensing of Tropospheric Aerosol over Dark Targets from MODIS: Collections 005 and 051: Revision 2; Feb 2009; 2009; p 96.

(19) Chin, M.; Ginoux, P.; Kinne, S.; Torres, O.; Holben, B. N.; Duncan, B. N.; Martin, R. V.; Logan, J. A.; Higurashi, A.; Nakajima, T. Tropospheric aerosol optical thickness from the GOCART model and comparisons with satellite and Sun photometer measurements. *J. Atmos. Sci.* **2002**, *59* (3), 461–483.

(20) Drury, E.; Jacob, D. J.; Spurr, R. J. D.; Wang, J.; Shinozuka, Y.; Anderson, B.; Clarke, A.; Dibb, J.; McNaughton, C.; Weber, R. Synthesis of satellite (MODIS), aircraft (ICARTT), and surface (IMPROVE, EPA-AQS, AERONET) aerosol observations over eastern North America to improve MODIS aerosol retrievals and constrain surface aerosol concentrations and sources. *J. Geophys. Res.* **2010**, *115* (D14204), 17 pp; DOI: 10.1029/2009JD012629.

(21) Hoff, R. M.; Christopher, S. A. Remote Sensing of Particulate Pollution from Space: Have We Reached the Promised Land. *J. Air Waste Manage. Assoc.* **2009**, *59* (6), 645–675.

(22) GEOS-Chem Aerosol Science Teem GEOS-Chem Aerosol Optics. http://www.atmos.colostate.edu/~heald/docs/GEOS_Chem_optics_description.pdf (accessed June 30, 2010).

(23) Zhang, Q.; Streets, D. G.; Carmichael, G. R.; He, K. B.; Huo, H.; Kannari, A.; Klimont, Z.; Park, I. S.; Reddy, S.; Fu, J. S.; Chen, D.; Duan, L.; Lei, Y.; Wang, L. T.; Yao, Z. L. Asian emissions in 2006 for the NASA INTEX-B mission. *Atmos. Chem. Phys.* **2009**, *9* (14), 5131–5153.

(24) Lei, Y.; He, K.-B.; Zhang, Q.; Liu, Z.-Y. Technology-based Emission Inventory of Particulate Matters (PM) from Cement Industry (in Chinese). *Environ. Sci.* **2008**, *29* (7), 336–341.

(25) Lei, Y.; Zhang, Q.; Nielsen, C. P.; He, K. An inventory of primary air pollutants and CO2 emissions from cement production in China, 1990–2020. *Submitted to Atmos. Environ.*

(26) Liu, Y.; Franklin, M.; Kahn, R.; Koutrakis, P. Using aerosol optical thickness to predict ground-level PM2.5 concentrations in the St. Louis area: A comparison between MISR and MODIS. *Remote Sens. Environ.* **2007**, *107* (1–2), 33–44.

(27) Choi, Y. S.; Ho, C. H.; Kim, J.; Gong, D. Y.; Park, R. J. The impact of aerosols on the summer rainfall frequency in China. *J. Appl. Meteorol. Climatol.* **2008**, *47* (6), 1802–1813.

(28) Gong, D. Y.; Ho, C. H.; Chen, D. L.; Qian, Y.; Choi, Y. S.; Kim, J. W. Weekly cycle of aerosol-meteorology interaction over China. *J. Geophys. Res., [Atmos.]* **2007**, *112* (D22202), 9 pp.

(29) Zhou, K.; Ye, Y. H.; Liu, Q.; Liu, A. J.; Peng, S. L. Evaluation of ambient air quality in Guangzhou, China. *J. Environ. Sci. (Beijing, China)* **2007**, *19* (4), 432–437.

(30) Choi, Y. S.; Ho, C. H.; Chen, D.; Noh, Y. H.; Song, C. K. Spectral analysis of weekly variation in PM10 mass concentration and meteorological conditions over China. *Atmos. Environ.* **2008**, *42* (4), 655–666.

(31) Choi, Y. S.; Park, R. J.; Ho, C. H. Estimates of ground-level aerosol mass concentrations using a chemical transport model with Moderate Resolution Imaging Spectroradiometer (MODIS) aerosol observations over East Asia. *J. Geophys. Res., [Atmos.]* **2009**, *114*, D04204, 15 pp.

(32) Boersma, K. F.; Eskes, H. J.; Veefkind, J. P.; Brinksma, E. J.; van der A, R. J.; Sneep, M.; van den Oord, G. H. J.; Levelt, P. F.; Stammes, P.; Gleason, J. F.; Bucsela, E. J. Near-real time retrieval of tropospheric NO2 from OMI. *Atmos. Chem. Phys.* **2007**, *7* (8), 2103–2118.

(33) Lin, J. T.; McElroy, M. B. Impacts of boundary layer mixing on pollutant vertical profiles in the lower troposphere: Implications to satellite remote sensing. *Atmos. Environ.* **2010**, *44* (14), 1726–1739.

(34) Lin, J. T.; McElroy, M. B.; Boersma, K. F. Constraint of anthropogenic NOx emissions in China from different sectors: a new methodology using multiple satellite retrievals. *Atmos. Chem. Phys.* **2010**, *10* (1), 63–78.

(35) Boersma, K. F.; Jacob, D. J.; Bucsela, E. J.; Perring, A. E.; Dirksen, R.; van der A, R. J.; Yantosca, R. M.; Park, R. J.; Wenig, M. O.; Bertram, T. H.; Cohen, R. C. Validation of OMI tropospheric NO2 observations during INTEX-B and application to constrain NOx emissions over the eastern United States and Mexico. *Atmos. Environ.* **2008**, *42* (19), 4480M−4497.

(36) Boersma, K. F.; Jacob, D. J.; Eskes, H. J.; Pinder, R. W.; Wang, J.; van der A, R. J. Intercomparison of SCIAMACHY and OMI tropospheric NO2 columns: Observing the diurnal evolution of chemistry and emissions from space. *J. Geophys. Res., [Atmos.]* **2008**, *113* (D16), 14 pp.

(37) Xu, X.; Lin, W.; Wang, T.; Yan, P.; Tang, J.; Meng, Z.; Wang, Y. Long-term trend of surface ozone at a regional background station in eastern China 1991−2006: enhanced variability. *Atmos. Chem. Phys.* **2008**, *8* (10), 2595–2607.

(38) Richter, A.; Burrows, J. P.; Nü ss, H.; Granier, C.; Niemeier, U. Increase in tropospheric nitrogen dioxide over China observed from space. *Nature* **2005**, *437* (1), 129–132.

(39) Wei, W. *Research and Forecast on Chinese Anthropogenic Emissions of Volatile Organic compounds*; Tsinghua University, Beijing, China, 2009.

ES101094T